Am J Transl Res 2022;14(8):5363-5378
www.ajtr.org /ISSN:1943-8141/AJTR0142839

Original Article

Role of the N6-methyladenosine regulatory factor in reducing the risk of cardiovascular disease: subtype diagnosis following aerobic exercise-assisted weight loss

Xiaoya Hao[1], Yukun Li[2], Guo Huang[2], Ying Zeng[2,3]

[1]College of Physical Education, University of South China, Hengyang, Hunan, China; [2]Hunan Province Key Laboratory of Cancer Cellular and Molecular Pathology, Cancer Research Institute, Hengyang Medical School, University of South China, Hengyang, Hunan, China; [3]School of Nursing, Hengyang Medical School, University of South China, Hengyang, Hunan, China

Received March 12, 2022; Accepted June 22, 2022; Epub August 15, 2022; Published August 30, 2022

Abstract: Objectives: This study aimed to construct a model based on different N6-methyladenosine (m6A) regulatory factors involved in reducing the risk of the development of cardiovascular diseases under conditions of aerobic exercise. Methods: We screened for significantly different expressions of m6A regulators from the GSE66175 dataset. Five candidate m6A regulators were identified using the random forest model to predict aerobic exercise-mediated fat loss and reduction of the risk of cardiovascular disease. A nomogram model was established for analysis, and the consensus clustering method was used to distinguish between the two m6A clusters (clusters A and B). The single-sample gene set-enrichment analysis method was used to assess the abundance of immune cells in the samples related to cardiovascular anomalies. We determined the relationship between the functions of 29 immune cells and m6A clusters. Results: Twelve significantly and differentially expressed m6A regulators in the control and aerobic exercise groups were screened out, and it was observed that METTL13 correlated positively with the expression levels of the YTH domain containing 1 (YTHDC1), YTH N (6)-methyl adenosine RNA binding protein 1, and leucine-rich pentatricopeptide repeat-containing. The fat mass and obesity-associated gene negatively correlated with YTHDC1 and the fragile X mental retardation 1 protein. The random forest and support vector machine models were used to screen the ELAV-like RNA binding protein 1 (*ELAVL1*), RNA binding motif protein 15B (*RBM15B*), insulin-like growth factor binding protein 1 (*IGFBP1*), Wilms tumor 1-associated protein (*WTAP*), and zinc finger CCCH-type containing 13 (*ZC3H13*) genes. Analysis of the line graph model and the results obtained using decision curve analysis revealed the efficiency of the model. Gene ontology enrichment analysis was used to analyze the m6A regulatory gene model, and the results suggested that it was associated with RNA splicing. The results obtained using the Kyoto Encyclopedia of Genes and Genomes enrichment analysis method suggests that the genes were associated with Alzheimer's disease and neurodegeneration pathways associated with multiple diseases. The m6A regulatory gene model was associated with most of the immune cells infiltrating tumors and was also closely related to genes associated with lipid metabolism. Conclusions: The m6A regulatory factor plays an important role in reducing the risk of cardiovascular disease under conditions of aerobic exercise-assisted weight loss. It is also associated with the metabolic pathways of low-density lipoprotein, high-density lipoprotein, and triglyceride.

Keywords: Cardiovascular disease, N6-methyladenosine (m6A), cluster subtypes

Introduction

Cardiovascular disease is currently the leading cause of global mortality [1]. The most common risk factors for cardiovascular disease are hypertension, diabetes, dyslipidemia, obesity, smoking, and age. These factors also influence the development and progress of atherosclerosis [2-5]. The reported incidence rates for central vascular disease are 35-40%, 75-78%, and >85% for people in the age group of 40-60 years, 60-80 years, and over 80 years, respectively [6]. Regular physical exercise helps improve physical function and prevents the

development of cardiovascular disease in the elderly. It also helps improve the quality of life [7].

N6-methyladenosine (m6A) modification is reported to be the most abundant messenger RNA (mRNA) modification in eukaryotes. Furthermore, m6A modification significantly influences the regulation of RNA processing, nucleation, splicing, and translation. It also dictates the stability achieved [8]. m6A modification is a dynamic process that can be reversed via regulation by a methylase and demethylase [9]. m6A modification plays an important regulatory role in the liver [10], gastric [11], lung [12], breast [13], and cervical [14] cancers and the development of other malignant tumors. It significantly influences the development process of the nervous [15] and reproductive [16] systems. The methyltransferase-like 14 (METTL14) can increase the level of expression of forkhead box O1 (FOXO1) by enhancing the extent of m6A modification. This, in turn, can induce the inflammation of endothelial cells and the formation of atherosclerotic plaque. Thus, METTL14 can be a potential target in the clinical treatment of atherosclerosis [17].

Physical exercise not only improves cardiovascular physiology but also addresses neck-related problems associated with cardiovascular diseases. Blood pressure and risk of coronary artery disease can be reduced, and blood lipid and insulin sensitivity can be improved through physical exercise [18, 19]. Additionally, physical exercise helps reduce the extent of sympathetic activity and achieve better control over blood pressure and heart rate [20, 21]. Population aging is increasing with each passing year, and the health and cognitive function of the elderly is being significantly improved through regular physical exercise [22]. It has been reported that physical activity is negatively correlated with the risk of long-term death, and the maximum survival benefit is realized when people exercise for approximately 150 minutes every week [23]. Furthermore, regular physical exercise can help temporarily decrease the risk of cardiovascular complications, acute myocardial infarction, heart failure, or stroke in patients with hypertension [24, 25].

We analyzed the GSE66175 database [26] and constructed a model based on candidate m6A regulatory factors that can predict the incidence rate of cardiovascular diseases under conditions of aerobic exercise. The results of this study are expected to better predict the influence of aerobic exercise on cardiovascular disease and help develop a guideline for follow-up treatment.

Materials and methods

Data acquisition

The GSE66175 dataset (consisting of 291 control group and 189 patients who performed aerobic exercise) was obtained from the Gene Expression Omnibus (GEO) database (https://www.ncbi.nlm.nih.gov/geo/query/acc.cgi?acc=GSE66175). Twenty-one m6A regulatory factors were extracted from the dataset. These regulators consisted of 8 methyltransferases (METTL14, ZC3H13, RBM15B, METTL3, WTAP, CBLL1, RBM15, and KIAA1429), 2 demethylases (FTO and ALKBH5), and 11 methylated reading proteins (ELAVL1, YTHDC1, YTHDF1, YTHDC2, YTHDF2, LRPPRC, HNRNPC, FMR1, YTHDF3, IGF2BP1, and HNRNPA2B1). These were extracted to analyze the difference between the m6A regulatory factors in the aerobic exercise and control groups and further determine their association with the risk of developing cardiovascular disease in the two groups.

Construction of the random forest model

The random forest (RF) and support vector machine (SVM) models were established as training models to predict whether regular aerobic exercise could reduce the risk of contracting cardiovascular disease. The “reverse cumulative distribution of residuals”, “box diagram of residuals”, and receiver operating characteristic (ROC) curves were generated to study the model. The RF model was developed using the “random forest” package (R statistical software) to screen the m6A regulatory factors that can predict whether aerobic exercise could reduce the risk of contracting cardiovascular disease. We set the ntrees and mtry at 100 and 3, respectively. Subsequently, we analyzed the importance of the 21 m6A regulatory factors under study and selected the appropriate m6A regulatory factors following the process of 10-fold cross-validation. SVM is a supervised machine learning algorithm based on the principles of structural risk minimization and the

Table 1. Lipid metabolism pathways related genes

Riginal Member	Gene Symbol	Gene Description
102465534	MIR6886	microRNA 6886
1071	CETP	cholesteryl ester transfer protein
19	ABCA1	ATP binding cassette subfamily A member
255738	PCSK9	proprotein convertase subtilisin
26119	LDLRAP1	low density lipoprotein receptor adap
302	ANXA2	annexin A2
335	APOA1	apolipoprotein A1
336	APOA2	apolipoprotein A2
338	APOB	apolipoprotein B
348	APOE	apolipoprotein E
3931	LCAT	lecithin-cholesterol acyltransferase
3949	LDLR	low density lipoprotein receptor
3990	LIPC	lipase C, hepatic type
4023	LPL	lipoprotein lipase
4547	MTTP	microsomal triglyceride transfer prot
9388	LIPG	lipase G, endothelial type
949	SCARB1	scavenger receptor class B member 1

framework of statistical learning theory. The changes in the m6A regulatory factors between the aerobic exercise and control groups can be better understood by identifying the best delamination.

Construction of the nomogram model

The "rms" R package was used to develop a nomogram model [27] based on the m6A regulatory factors. The model was used to predict the incidence rates of cardiovascular events. Calibration curves were analyzed to study the accuracy and consistency of the predicted values and determine the agreement of the predicted values with the actual values. The decision curve analysis (DCA) method [28] was used to analyze the intervention effect of the m6A regulatory factors. The clinical impact curve was generated to evaluate whether the decision-making ability of the model could be exploited to reduce the incidence rate of cardiovascular disease.

Identification of molecular subtypes by analyzing m6A regulatory factors

The "consensus clustering +" software package associated with R was used for identifying the molecular subtypes. The consensus clustering method was used to determine and study the different m6A patterns.

Identification of differentially expressed genes (DEGs) among different m6A patterns and analysis of gene function enrichment

The DEGs between different m6A patterns were screened using the "limma" (R) package. P<0.001 was set as the screening criteria. The "cluster analyzer" package belonging to the R software was used for Gene Ontology (GO) and Kyoto Encyclopedia of Genes and Genomes (KEGG) [29] function enrichment analysis to unearth the possible mechanisms associated with the occurrence of cardiovascular events. The enrichment circle diagram was used to visualize the results.

Characteristics of the m6A regulatory factor-related genes

The principal component analysis (PCA) algorithm [30] was used to evaluate the m6A score of each sample and quantify the m6A pattern. PCA was used to distinguish between different m6A modes. Subsequently, the m6A score was calculated as follows: m6A score = PC1i, where PC1 represents the principal component 1, and i indicates the expression levels of the DEGs.

Infiltration of immune cells

The abundance of the immune cells associated with cardiovascular anomalies was determined following the ssGSEA method [31]. "GSEAbase" (R package) was used for ssGSEA, and the functions of 29 immune cells and m6A patterns were studied. The enrichment of the gene was studied, and the abundance of the immune cells in each sample set was determined.

Role of lipid metabolism pathways in m6A clustering

The genes associated with lipid metabolism (M39747) (**Table 1**) were downloaded from the GSEA database (http://www.gsea-msigdb.org/gsea/msigdb/search.jsp). Following this, the expression levels of the genes associated with lipid metabolism pathways and m6A cluster

and gene clusters were studied. Subsequently, the relationship between the genes associated with the lipid metabolism pathways and different types of m6A regulators was determined.

Statistical analyses

The linear regression analysis method was used to explore the correlation between the m6A regulators. Kruskal-Wallis test was conducted to understand the differences between the two groups. All the parameters were analyzed using a two-tailed test. $P<0.05$ was considered to be statistically significant. R (version 4.0.3) was used for all statistical analyses.

Results

Expression levels of the 21 m6A regulatory factors

The differential expression levels of the 21 m6A regulatory factors associated with the aerobic exercise and control groups were analyzed using the "limma" package (R software). Twelve m6A regulatory factors (WTAP, ZC3H13, RBM15, RBM15B, CBLL1, YTHDC1, YTHDC2, YTHDF1, YTHDF2, IGFBP1, IGFBP2, and ELAVL1) with significantly different levels of expression were screened and visualized using heat maps and histograms. Compared with the control group, RBM15, RBM15B, YTHDC2, YTHDF1, YTHDF2, and IGFBP were increased in the aerobic exercise group. It was observed that the expression levels of the other m6A regulatory factors decreased in the control group (**Figure 1A**, **1B**).

Correlation between the different m6A regulatory factors

We used the linear regression analysis method to explore the correlation between the 21 m6A regulatory factors and the occurrence of cardiovascular diseases under conditions of aerobic exercise. We found that METTL13 correlated positively with the expression levels of YTHDC1, YTHDF1, and LRPPRC. FTO was found to correlate negatively with YTHDC1 and FMR1 (**Figure 1C-G**).

Construction of the RF and SVM models

The "reverse cumulative distribution of residuals" (**Figure 2A**) and "residual profile" (**Figure 2B**) of the RF and SVM models were analyzed, and the results revealed that the smallest residual was obtained for the RF model. The model was studied and analyzed further by simultaneously generating and analyzing the ROC curve. The results obtained using the RF model were more accurate than those obtained using the SVF model (**Figure 2C**). The sample residual associated with the RF model was small, indicating the efficiency of the model. Furthermore, the most accurate predictions for cardiovascular events could be obtained using the RF model. Thus, suggesting that it was the better predictive model of the two models analyzed. The genes were ranked based on their importance, and 21 m6A regulators were visualized (**Figure 2D**). The 10-fold cross-validation method was used for sample analysis, which revealed that the maximum accuracy in selecting the top 12 m6A regulators could be achieved using the RF model. The top 5 m6A regulators [ELAV-like RNA binding protein 1 (ELAVL1), RNA binding motif protein 15B (RBM15B), insulin-like growth factor binding protein 1 (IGFBP1), Wilms tumor 1 associated protein (WTAP), and zinc finger CCCH-type containing 13 (ZC3H13)] were further analyzed as potential candidate genes (**Figure 2E**).

Construction of the nomograph model

A nomogram model consisting of 12 candidate m6A regulators was developed using the "rms" R package. The model was used to predict the incidence rate of cardiovascular events (**Figure 3A**). Analysis of the calibration curve revealed that the predictive ability of the nomogram model is good (**Figure 3B**). The red line spanning the region 0-1 in the DCA curve lies above the gray and black lines, which revealed the decision-making power of the nomogram model. It was observed that regular aerobic exercise helps reduce the incidence of cardiovascular diseases (**Figure 3C**). Analysis of the clinical impact curve revealed that the nomogram model could be efficiently used to predict the outcome with high accuracy (**Figure 3D**).

Establishment of the m6A mode

Two m6A patterns were identified following the consensus clustering method using the "Consensus Cluster" R software package (based on 12 significant m6A regulatory fac-

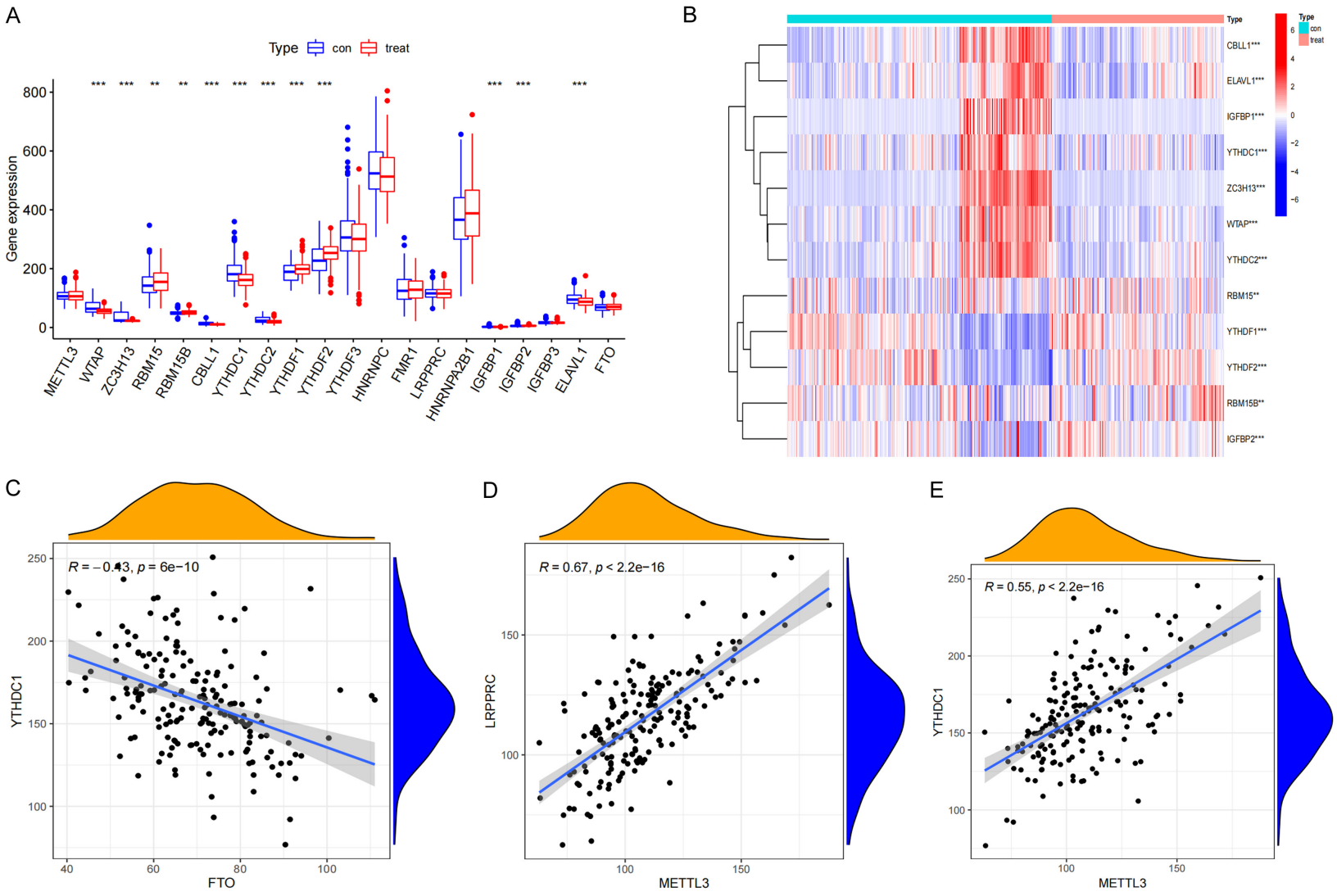
A
Type con treat
Gene expression
METTL3 WTAP ZC3H13 RBM15 RBM15B CBLL1 YTHDC1 YTHDC2 YTHDF1 YTHDF2 YTHDF3 HNRNPC FMR1 LRPPRC HNRNPA2B1 IGFBP1 IGFBP2 IGFBP3 ELAVL1 FTO
B
Type
CBLL1*** ELAVL1*** IGFBP1*** YTHDC1*** ZC3H13*** WTAP*** YTHDC2*** RBM15** YTHDF1*** YTHDF2*** RBM15B** IGFBP2***
C
R = −0.43, p = 6e−10
YTHDC1
FTO
D
R = 0.67, p < 2.2e−16
LRPPRC
METTL3
E
R = 0.55, p < 2.2e−16
YTHDC1
METTL3

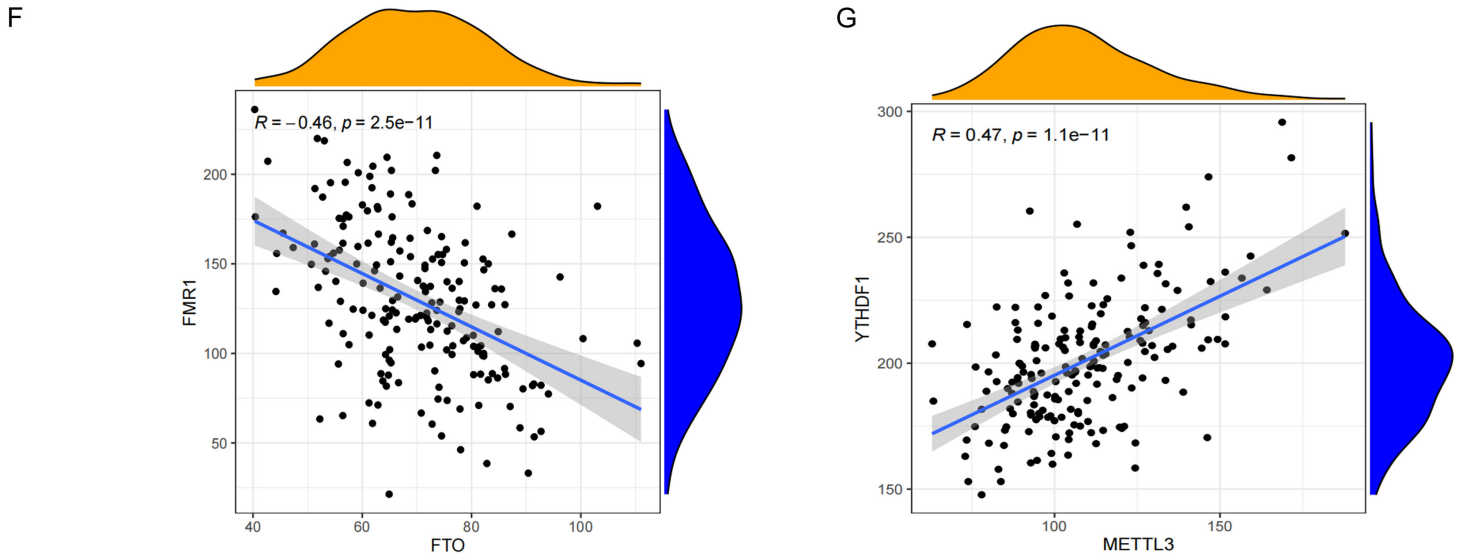

Figure 1. The 21 m6A regulatory factors expression and correlation. A. Expression heat map of 21 m6A regulators in the aerobic exercise group and control group. B. Differences between 21 m6A regulators in the aerobic exercise group and the control group express histogram. C. Correlation of FTO with YTHDC1. D. Correlation of METTL3 with LRPPRC. E. Correlation of METTL3 with YTHDC1. F. Correlation of FTO with FMR1. G. Correlation of METTL3 with TYTHDF1.

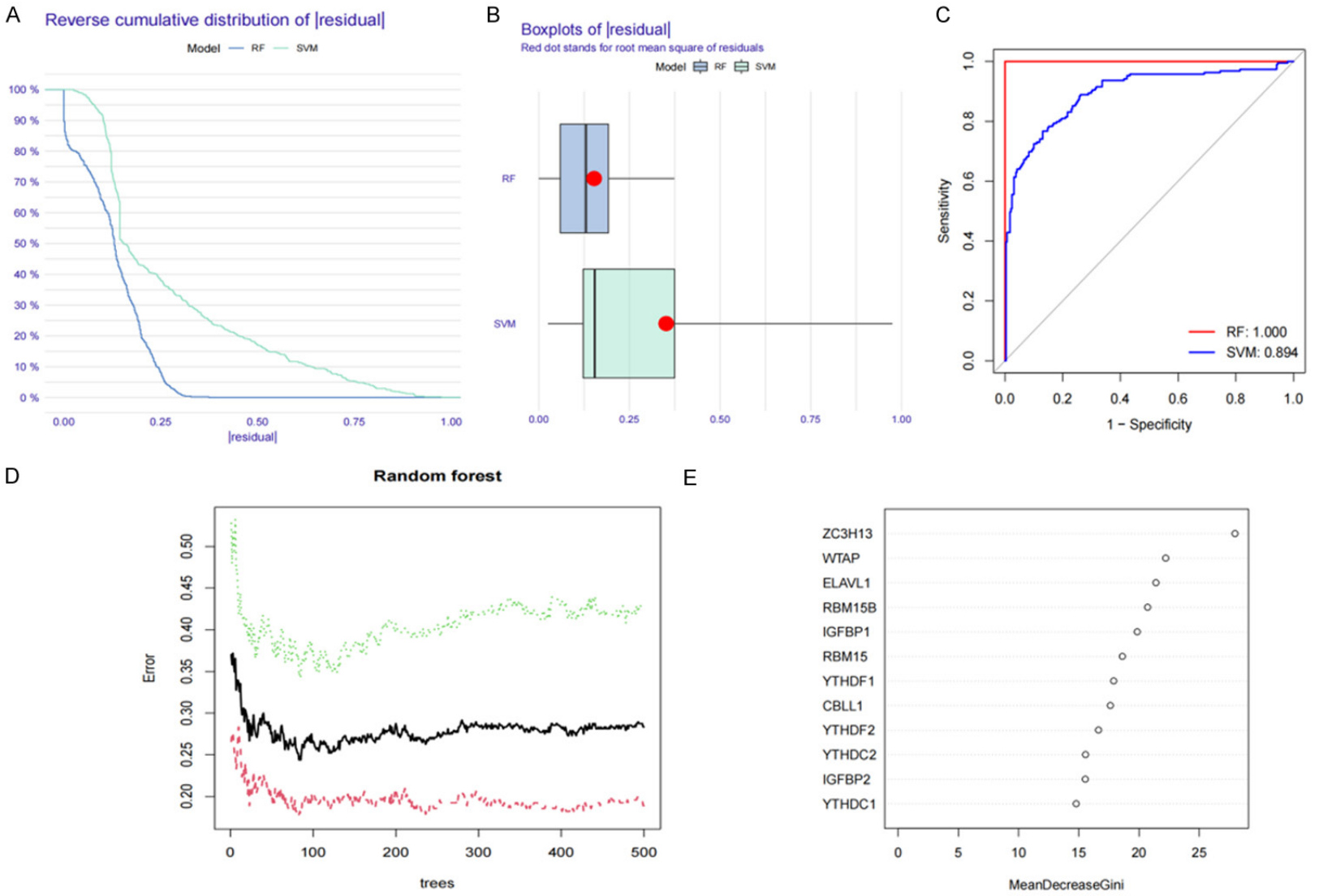

Figure 2. Random forest (RF) model construction. A. Reverse cumulative distribution of residual was plotted to show the residual distribution of RF and support vector machine (SVM) model. B. Boxplots of residual was plotted to show the residual distribution of RF and SVM model. C. ROC curves indicated the accuracy of the RF and SVM model. D. A 10-fold cross-validation curve was used to assess the quality of cardiovascular events predicted by aerobic exercise in RF models. The green line indicates the error of the experimental group, the black line indicates the error of the sample, and the red line controls the error. E. The importance of the 21 m6A regulatory factors based on the RF model.

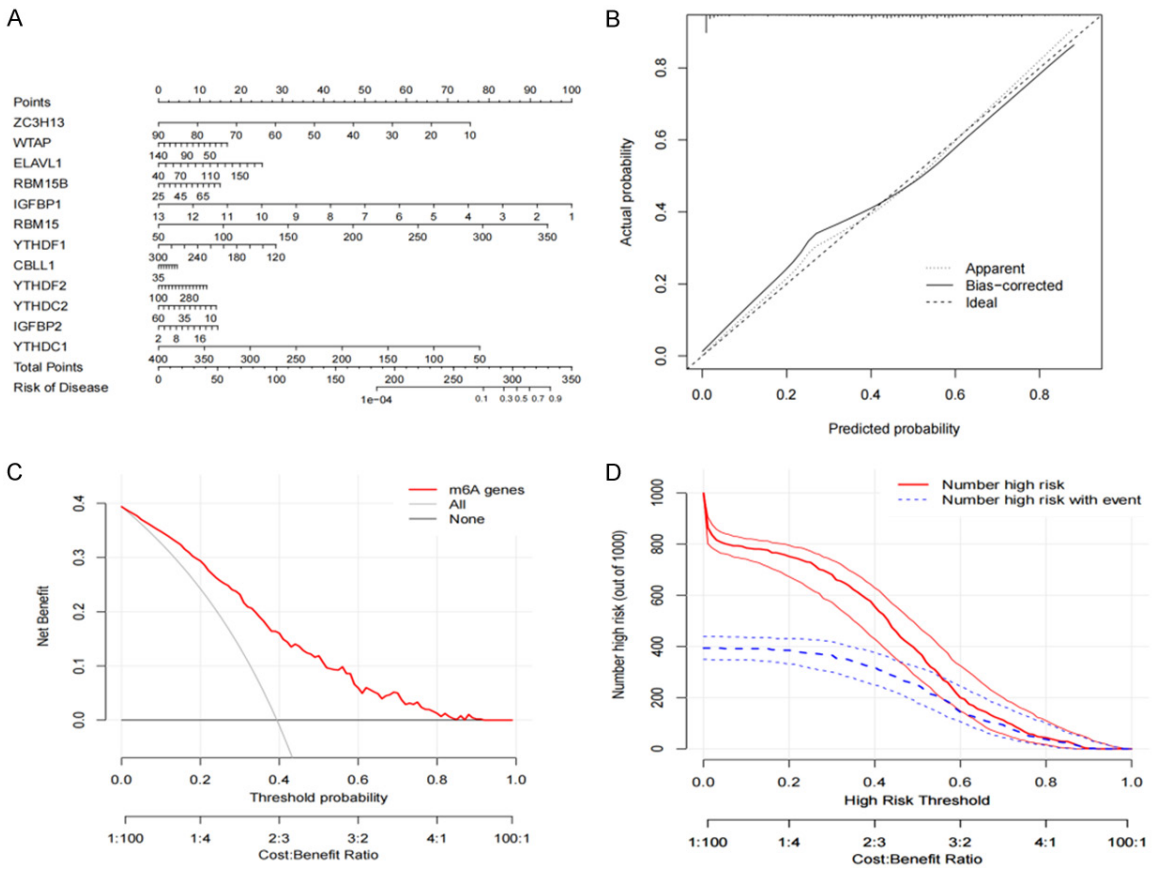

Figure 3. Construction of a nomogram model. A. nomogram model based on 12 candidate m6A regulatory factors. B. The predictive power of the nomogram model displayed by calibrating the curve. C. Decision-making based on the line chart model to prevent cardiovascular events. D. Evaluate the clinical impact of the line chart model by clinical impact curve.

tors; **Figure 4A**). Cluster A consisted of 109 cases, and cluster B consisted of 80 cases. The differential expression heat map (**Figure 4B**) and histogram (**Figure 4C**) of the m6A regulatory factors belonging to the two clusters were generated. The expression levels of WTAP, ZC3H13, RBM15, YTHDC1, YTHDC2, YTHDF2, and IGFBP1 in cluster A were higher than those in cluster B. The expression levels of RBM15B, IGFBP2, and ELAVL1 in cluster A were lower than those in cluster B. There was no significant difference in the expression levels of CBLL1 and YTHDF1 between clusters A and B. The results obtained using the PCA method revealed that the two m6A patterns could be distinguished efficiently using the 12 significant m6A regulators (**Figure 4D**). Under the two m6A modes, a total of 400 DEGs related to m6A were selected. We used the GO and KEGG functional enrichment analysis methods to understand the enrichment of these DEGs in the cases of cardiovascular diseases. The results were visualized using a circle diagram representing enrichment (**Figure 4E**). It was observed that these DEGs were primarily enriched in GO: 0008380, GO: 0000377, and GO: 0000398, which were associated with the process of RNA splicing. The KEGG pathway was found to be primarily enriched in hsa05022 (neurodegeneration - pathway of multiple diseases) and hsa05010 (Alzheimer's disease) (**Figure 4F**).

We determined the abundance of immune cells in the cardiovascular-event samples following the ssGSEA method and investigated the correlation between the 12 significant m6A regulators and the immune cells. We observed that an m6A methyltransferase (RBM15) correlated negatively with various immune cells (**Figure 5A**). We also studied the differences in the extent of immune cell infiltration realized in patients with high and low expression levels of RBM15. Improved immune functions were

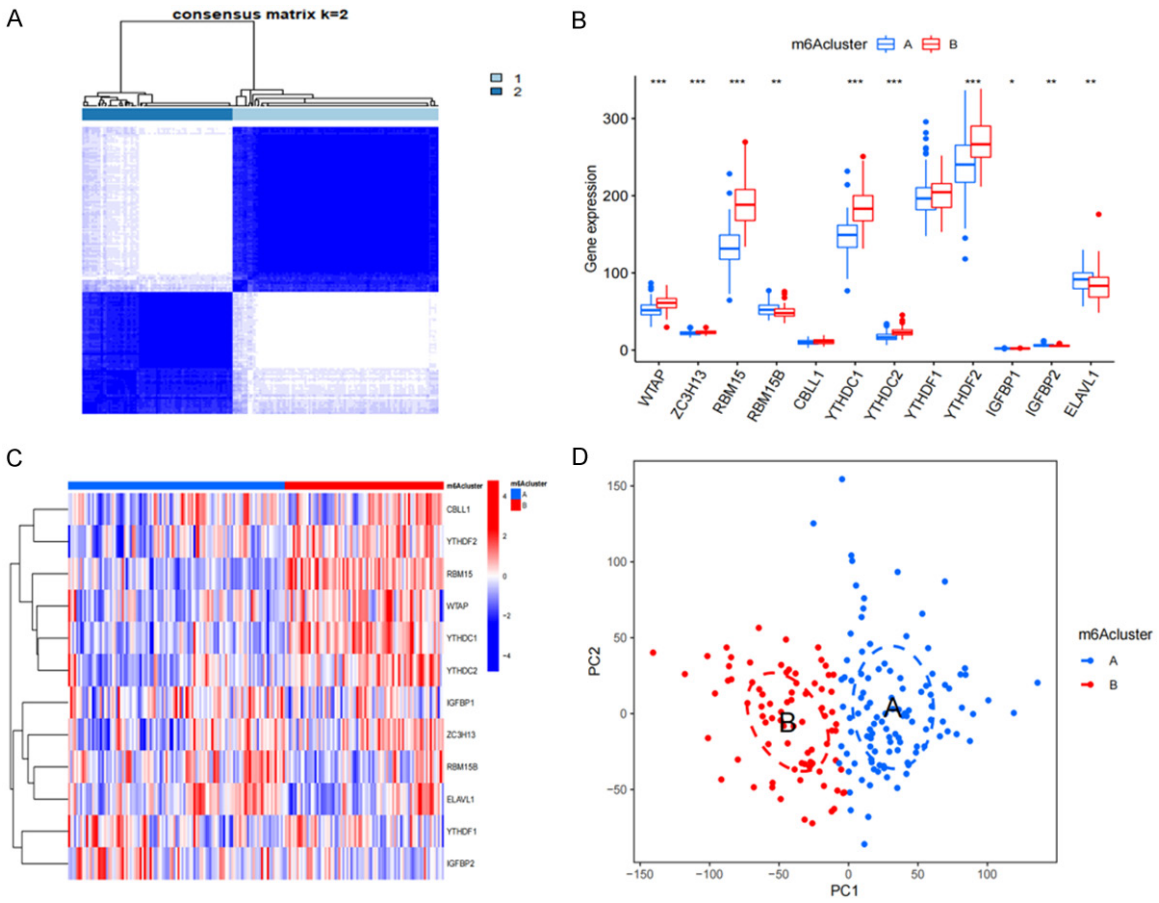

Figure 4. Clustering of 12 significant m6A regulators. A. Consensus matrix for 12 significant m6A regulators of k=2. B. Heat map of the expression of 12 significant m6A regulators in cluster A and cluster B. C. Histogram of differential expression of 12 significant m6A regulators in cluster A and cluster B. D. The expression profiles of 12 significant m6A regulators were analyzed by principal components, showing significant differences in the transcriptome between the two m6A modes.

observed in patients with low expression levels of RBM15 (**Figure 5B**). Examination of the extent of immune cell infiltration associated with the two m6A patterns indicated that cluster A was associated with Th1-dominant immunity, while cluster B was associated with $CD8^+$ T cell, $CD4^+$ T cell, γ T cell, immature B cell, and type 2 helper T cell-dominant immunity (**Figure 5C**). These findings suggest that the incidence of cardiovascular disease can potentially correlate with T cell immunity.

Identification of two different m6A gene patterns and analysis of m6A gene characteristics

The consensus clustering method was used to construct gene clusters A and B based on the 400 DEGs related to m6A to further verify the m6A pattern. The patterns were consistent with the grouping patterns of the m6A gene (**Figure 6A**). Significant differences were observed between the expression levels of the 12 significant m6A regulatory factors belonging to gene clusters A and B (**Figure 6B**) and immune cell infiltration (**Figure 6C**). Sankey diagram was used to visualize the relationship between the m6A pattern, m6A gene pattern, and m6A score (**Figure 6D**). The heat map representing the expression data corresponding to the 400 m6A-related DEGs belonging to the gene clusters A and B is presented in **Figure 6E**.

Role of the m6A model in the development of cardiovascular disease

We studied the relationship between the m6A cluster, m6A gene cluster, and m6A score to understand the influence of these patterns on the development of cardiovascular disease. It was found that the score of cluster A was high

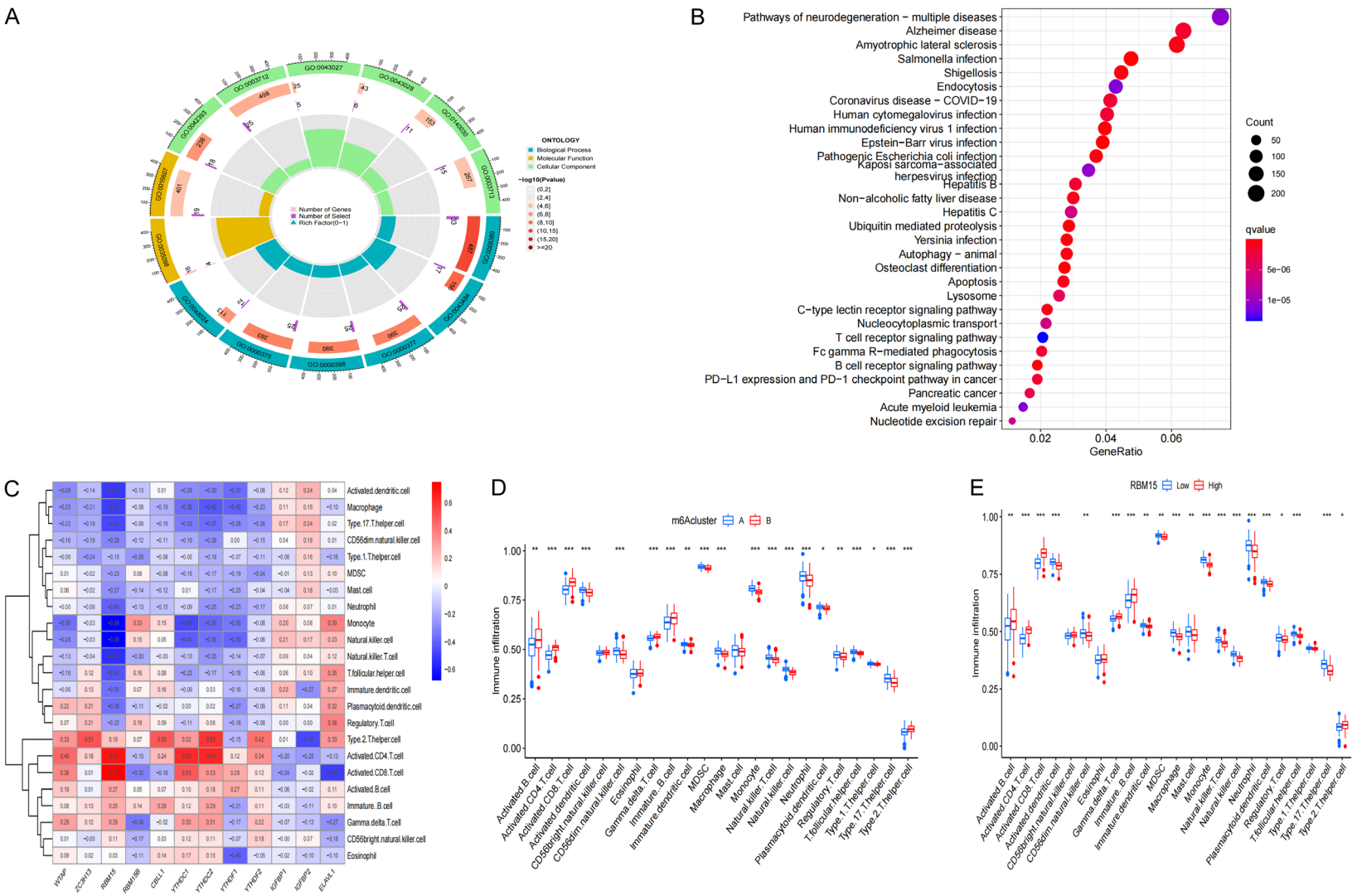

Figure 5. Functional enrichment analysis. (A) GO enrichment analysis. (B) KEGG enrichment analysis. (C) Correlation between 12 m6A regulators and immune cell infiltration. (D) Differences between high and low RBM15 expression and immune cell infiltration. (C) Differences in immune cell infiltration (E) m6A subtypes and immune cell infiltration in clusters A and B.

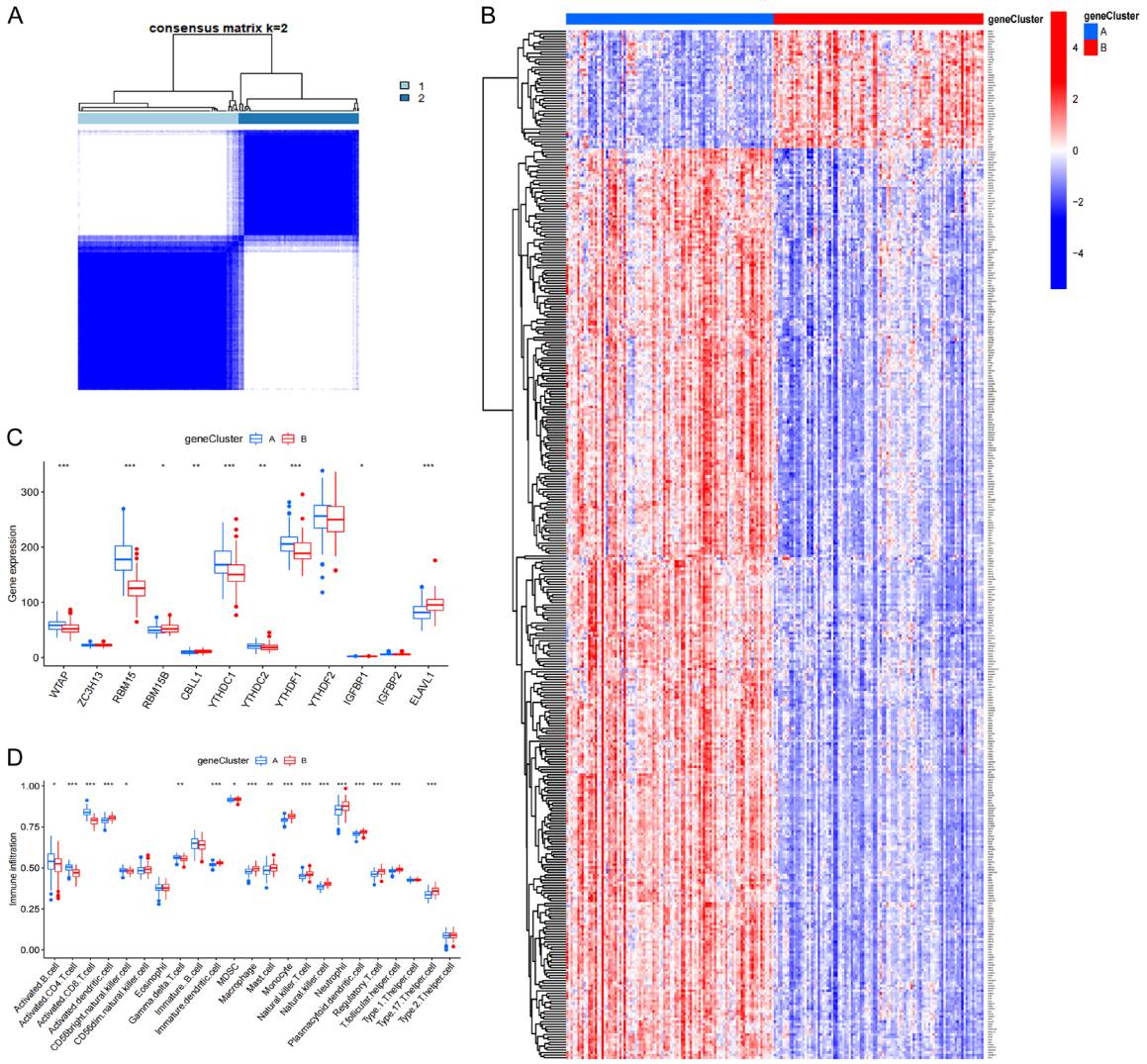

Figure 6. Gene clustering of m6A-related DEGs. A. Consensus matrix of DEGs associated with 400 m6A of k=2. B. Heat map of expression of DEGs in gene cluster A and gene cluster B. C. Immune cell infiltrates between gene cluster A and gene cluster B. D. Differences between cluster A and cluster B and gene clusters.

for the m6A cluster (**Figure 7A**), while that of cluster B was high for the m6A gene cluster (**Figure 7B**). The m6A clusters and gene clusters are mostly in low m6A scores (**Figure 7C**). The m6A cluster and gene cluster were found to correlate with the expression of *ANXA2*, *APOA1*, *APOE*, *CETP*, *LCAT*, *LDLR*, *LIPC*, and *SCARB1* (**Figure 7D**, **7E**).

Discussion

Congenital heart disease (CHD), arrhythmia, myocardial hypertrophy, heart failure, stroke, and vascular diseases fall under the category of cardiovascular diseases. According to the data revealed by the World Health Organization (WHO), nearly 18 million people died of cardiovascular diseases in 2019, accounting for 32% of the global death toll. Moreover, this number is expected to increase to more than 23 million by 2030 [32]. Differential expression analysis of 21 m6A regulatory factors from the GSE66175 dataset identified 12 genes that were selected to construct the RF and SVM models. A nomogram model was also constructed based on the 12 candidate m6A regulatory factors. Analysis of the DCA curve helped in decision-making. The process was based on the nomogram model, and the results revealed that regular aerobic exercise reduced the incidence rate of cardiovascular diseases. The five most important m6A regula-

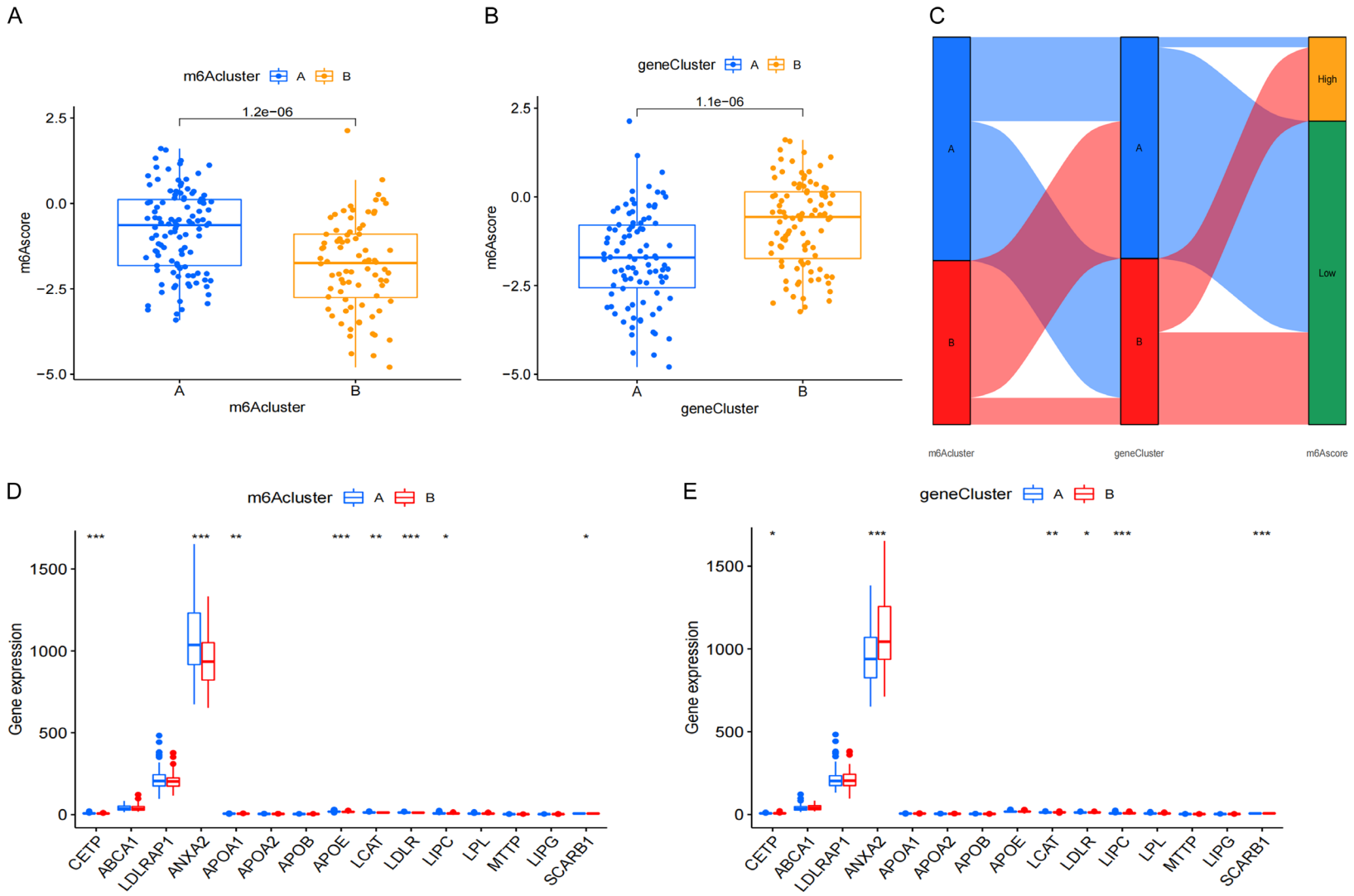

Figure 7. The role of m6A clustering in predicting the occurrence of cardiovascular events. A. Difference m6A score between m6A cluster A and cluster B. B. Differences m6A scores between gene cluster A and gene cluster B. C. The Sankey plot shows the relationship between m6A cluster, gene cluster, and m6A scores. D. ANXA2, APOA1, APOE, CETP, LCAT, LDLR, LIPCHE and SCARB1 differential expression levels between m6A cluster A and cluster B. E. Differences in expression levels of ANXA2, APOA1, APOE, CETP, LCAT, LDLR, LIPC and SCARB1 between gene cluster A and gene cluster B. *P<0.05, **P<0.01, and ***P<0.001.

tory factors (ELAVL1, RBM15B, IGFBP1, WTAP, and ZC3H13) were selected as candidate genes to predict the preventive effect of aerobic exercise. ELAVL1 is widely expressed in RNA-binding proteins, and it binds to rich AU elements and U-rich elements to stabilize mRNA. In mice with IL-10 deletion, down-regulation of ELAVL1 could mimic an anti-inflammatory response. Under these conditions, inflammatory response and left ventricular dysfunction could be attenuated post-myocardial infarction [33]. ELAVL1 promotes gene expression by binding to 3'UTR of VEGF-A and TNFα, which is involved in angiogenesis, apoptosis, and inflammatory processes [34]. Knockout of the *ELAVL1* gene can potentially reduce the inflammatory response during myocardial infarction [35]. MiR-133a is enriched in exosomes of Cardiac fibroblasts secrete (CFs) and transported to cardiomyocytes wherein ELAVL1 is modulated to inhibit pyroptosis [36]. ELAVL1 is believed to be an important factor that regulates cardiovascular diseases. IGFBP1 levels are inversely proportional to the risk of developing cardiovascular disease, the thickness of the carotid intima-media, and the incidence of macrovascular disease [37]. When the rat model of defective reperfusion injury was studied, it was found that the injection of shRNA-WTAP into the anterior wall of the left ventricle could significantly inhibit the processes of m6A modification, generation of endoplasmic reticulum stress, and apoptosis under conditions of defective reperfusion injury. This confirmed that WTAP played a key role in the occurrence of myocardial infarction [38]. ZC3H13 is an m6A methyltransferase that is a potential regulator of nuclear m6A methylation. It also regulates the self-renewal of mouse embryonic stem cells [39]. ZC3H13 inhibits the progression of liver cancer and enhances chemosensitivity through MA-PKM 2-mediated glycolysis [40]. ZC3H13 can potentially inhibit the proliferation and invasion of colorectal cancer by blocking the RAS-ERK signaling pathway [41]. A few researchers have studied the relationship between these five candidate m6A regulatory factors and cardiovascular diseases and reported the results. We hope that the results presented herein can further provide a platform for the conduction of experimental research on these m6A regulatory factors.

Cardiovascular disease is closely associated with lipid metabolism. Genes related to the metabolic pathways of low-density lipoprotein, high-density lipoprotein (HDL), and TG were selected for analysis. We observed differences in expression of ANXA2, APOA1, APOE, CETP, LCAT, LDLR, LIPC, and SCARB1 in the m6A cluster and gene cluster. APOA1 is the primary structural protein associated with HDL. It accounts for approximately 70% of the HDL proteins and mediates a variety of anti-atherosclerotic functions associated with HDL [42]. Physical exercise could induce polymorphism in the *APOE* gene and reduce the incidence rate of cardiovascular diseases as well as the associated mortality rate [43]. The liposome associated with HDL (CETP) and metabolic syndrome functions can be altered by losing weight and exercising. The functions of HDL can be improved, and the incidence rate of cardiovascular diseases can be reduced under these conditions [44]. Lecithin-cholesterol acyltransferase (LCAT) participates in the process of synthesis of cholesterol esters and plays an important role in the metabolism of HDL. High-intensity physical exercise can reverse the transport of cholesterol and prevent atherosclerosis [45]. Physical exercise helps increase the expression levels of the *LDLR* and *PCSK 9* genes (associated with the excretion of intestinal cholesterol) in the intestine [46]. Physical activity alters the effects of *LPL*, *LIPC*, and *CETP* polymorphism on the HDL-C levels and myocardial infarction risk in European women [47]. Polymorphism of the *SCARB1* gene was studied, and it was observed that the SCARB1AA genotype reduced the risk of contracting cardiovascular diseases, while the GA genotype and G allele increased the risk of coronary heart disease; carriers with the AA genotype were characterized by high levels of HDL subfractions [48].

In conclusion, this study established a model based on m6A regulatory factors to predict the lowering of risk of cardiovascular events through aerobic exercise. We further identified two m6A patterns in which the m6A cluster (clusterA) may reduce cardiovascular events by regulating lipid metabolism involved in aerobic exercise.

Acknowledgements

This study was funded by Excellent Youth Project of Hunan Provincial Department of Education, Grant/Award number: 19B495; Hunan Excellent Young Teachers Fund, Grant/Award number: 2018191RQG010.

Disclosure of conflict of interest

None.

Address correspondence to: Guo Huang and Ying Zeng, Hunan Province Key Laboratory of Cancer Cellular and Molecular Pathology, Cancer Research Institute, Hengyang Medical School, University of South China, Hengyang, Hunan, China. E-mail: huangguo@usc.edu.cn (GH) zengying2003@126.com (YZ)

References

[1] Whelton P and Colantonio L. Cardiovascular disease risk estimation in China. Ann Intern Med 2019; 170: 340-341.

[2] Kaze A, Santhanam P, Erqou S, Ahima R, Bertoni A and Echouffo-Tcheugui J. Body weight variability and risk of cardiovascular outcomes and death in the context of weight loss intervention among patients with type 2 diabetes. JAMA Netw Open 2022; 5: e220055.

[3] Heath L, Jebb S, Aveyard P and Piernas C. Obesity, metabolic risk and adherence to healthy lifestyle behaviours: prospective cohort study in the UK Biobank. BMC Med 2022; 20: 65.

[4] Santos R. Calcified and noncalcified coronary plaques and atherosclerotic cardiovascular events in patients with severe hypercholesterolemia-moving forward with risk stratification and therapy. JAMA Netw Open 2022; 5: e2148147.

[5] Yang Y, Peng N, Chen G, Wan Q, Yan L, Wang G, Qin Y, Luo Z, Tang X, Huo Y, Hu R, Ye Z, Qin G, Gao Z, Su Q, Mu Y, Zhao J, Chen L, Zeng T, Yu X, Li Q, Shen F, Chen L, Zhang Y, Wang Y, Deng H, Liu C, Wu S, Yang T, Li M, Xu Y, Xu M, Zhao Z, Wang T, Lu J, Bi Y, Wang W, Ning G, Zhang Q and Shi L. Interaction between smoking and diabetes in relation to subsequent risk of cardiovascular events. Cardiovasc Diabetol 2022; 21: 14.

[6] Van't Hof J, Duval S, Luepker R, Jones C, Hayes S, Cooper L, Patten C and Brewer L. Association of cardiovascular disease risk factors with sociodemographic characteristics and health beliefs among a community-based sample of African American adults in minnesota. Mayo Clin Proc 2022; 97: 46-56.

[7] Yerramalla M, McGregor D, van Hees V, Fayosse A, Dugravot A, Tabak A, Chen M, Chastin S and Sabia S. Association of daily composition of physical activity and sedentary behaviour with incidence of cardiovascular disease in older adults. Int J Behav Nutr Phys Act 2021; 18: 83.

[8] Wiener D and Schwartz S. The epitranscriptome beyond mA. Nat Rev Genet 2021; 22: 119-131.

[9] Jiang X, Liu B, Nie Z, Duan L, Xiong Q, Jin Z, Yang C and Chen Y. The role of m6A modification in the biological functions and diseases. Signal Transduct Target Ther 2021; 6: 74.

[10] Rong D, Wu F, Lu C, Sun G, Shi X, Chen X, Dai Y, Zhong W, Hao X, Zhou J, Xia Y, Tang W and Wang X. m6A modification of circHPS5 and hepatocellular carcinoma progression through HMGA2 expression. Mol Ther Nucleic Acids 2021; 26: 637-648.

[11] Zhou Y, Wang Q, Deng H, Xu B, Zhou Y, Liu J, Liu Y, Shi Y, Zheng X and Jiang J. N6-methyladenosine demethylase FTO promotes growth and metastasis of gastric cancer via mA modification of caveolin-1 and metabolic regulation of mitochondrial dynamics. Cell Death Dis 2022; 13: 72.

[12] Jiang F, Hu Y, Liu X, Wang M and Wu C. Methylation pattern mediated by mA regulator and tumor microenvironment invasion in lung adenocarcinoma. Oxid Med Cell Longev 2022; 2022: 2930310.

[13] Petri B, Piell K, South Whitt G, Wilt A, Poulton C, Lehman N, Clem B, Nystoriak M, Wysoczynski M and Klinge C. HNRNPA2B1 regulates tamoxifen- and fulvestrant-sensitivity and hallmarks of endocrine resistance in breast cancer cells. Cancer Lett 2021; 518: 152-168.

[14] Ma X, Li Y, Wen J and Zhao Y. m6A RNA methylation regulators contribute to malignant development and have a clinical prognostic effect on cervical cancer. Am J Transl Res 2020; 12: 8137-8146.

[15] Li M, Zhao X, Wang W, Shi H, Pan Q, Lu Z, Perez S, Suganthan R, He C, Bjørås M and Klungland A. Ythdf2-mediated mA mRNA clearance modulates neural development in mice. Genome Biol 2018; 19: 69.

[16] Lin Z, Hsu P, Xing X, Fang J, Lu Z, Zou Q, Zhang K, Zhang X, Zhou Y, Zhang T, Zhang Y, Song W, Jia G, Yang X, He C and Tong M. Mettl3-/Mettl14-mediated mRNA N-methyladenosine modulates murine spermatogenesis. Cell Res 2017; 27: 1216-1230.

[17] Jian D, Wang Y, Jian L, Tang H, Rao L, Chen K, Jia Z, Zhang W, Liu Y, Chen X, Shen X, Gao C, Wang S and Li M. METTL14 aggravates endothelial inflammation and atherosclerosis by increasing FOXO1 N6-methyladeosine modifications. Theranostics 2020; 10: 8939-8956.

[18] Rees-Punia E, Patel A, Nocera J, Chantaprasopsuk S, Demark-Wahnefried W, Leach C, Smith T, Cella D and Gapstur S. Self-reported physical activity, sitting time, and mental and physical health among older cancer survivors compared with adults without a history of cancer. Cancer 2020; 127: 115-123.

[19] Ko G, Davidson L, Brennan A, Lam M and Ross R. Abdominal adiposity, not cardiorespiratory fitness, mediates the exercise-induced change

in insulin sensitivity in older adults. PLoS One 2016; 11: e0167734.
[20] Betageri O, Al-Turk B, Freeman A and Aggarwal M. Prevention and reversal of morbidity in today's cardiovascular patient: role of lifestyle modification and nutrition in the current era. Curr Cardiol Rep 2021; 23: 143.
[21] Gu C, Yan J, Zhao L, Wu G and Wang Y. Regulation of mitochondrial dynamics by aerobic exercise in cardiovascular diseases. Front Cardiovasc Med 2021; 8: 788505.
[22] Sanchis-Soler G, Tortosa-MartMart J, Manchado-Lopez C and Cortell-Tormo J. The effects of stress on cardiovascular disease and Alzheimer's disease: physical exercise as a counteract measure. Int Rev Neurobiol 2020; 152: 157-193.
[23] Higueras-Fresnillo S, Cabanas-Snillo S, Cabanas-SSas-Sascular disease jo I, Banegas J, Sadarangani K, Rodrani K, Artalejo F and Martinez-Gomez D. Physical activity and association between frailty and all-cause and cardiovascular mortality in older adults: population-based prospective cohort study. J Am Geriatr Soc 2018; 66: 2097-2103.
[24] Nagata J, Vittinghoff E, Pettee Gabriel K, Garber A, Moran A, Sidney S, Rana J, Reis J and Bibbins-Domingo K. Physical activity and hypertension from young adulthood to middle age. Am J Prev Med 2021; 60: 757-765.
[25] Endo M, Fujihara C, Miura A, Kashima H and Fukuba Y. Effects of meal ingestion on blood pressure and regional hemodynamic responses after exercise. J Appl Physiol (1985) 2016; 120: 1343-1348.
[26] Blackburn H, McErlean S, Jellema G, van Laar R, Vernalis M and Ellsworth D. Gene expression profiling during intensive cardiovascular lifestyle modification: relationships with vascular function and weight loss. Genom Data 2015; 4: 50-53.
[27] Balachandran VP, Gonen M, Smith JJ and DeMatteo RP. Nomograms in oncology: more than meets the eye. Lancet Oncol 2015; 16: e173-180.
[28] Li J, Cao J, Li P, Yao Z, Deng R, Ying L and Tian J. Construction of a novel mRNA-signature prediction model for prognosis of bladder cancer based on a statistical analysis. BMC Cancer 2021; 21: 858.
[29] Kanehisa M, Furumichi M, Sato Y, Ishiguro-Watanabe M and Tanabe M. KEGG: integrating viruses and cellular organisms. Nucleic Acids Res 2021; 49: D545-D551.
[30] Abbas LF, Joseph AK, Day J, Cole NA, Hallac R, Derderian C and Jacobe HT. Revealing novel, latent subsets of morphea patients through principal component analysis. J Am Acad Dermatol 2022: 186: 193-195.
[31] Subramanian A, Tamayo P, Mootha VK, Mukherjee S, Ebert BL, Gillette MA, Paulovich A, Pomeroy SL, Golub TR, Lander ES and Mesirov JP. Gene set enrichment analysis: a knowledge-based approach for interpreting genome-wide expression profiles. Proc Natl Acad Sci U S A 2005; 102: 15545-15550.
[32] Roth G, Johnson C, Abajobir A, Abd-Allah F, Abera S, Abyu G, Ahmed M, Aksut B, Alam T, Alam K, Alla F, Alvis-Guzman N, Amrock S, Ansari H, Ärnlöv J, Asayesh H, Atey T, Avila-Burgos L, Awasthi A, Banerjee A, Barac A, Bärnighausen T, Barregard L, Bedi N, Belay Ketema E, Bennett D, Berhe G, Bhutta Z, Bitew S, Carapetis J, Carrero J, Malta D, Castañeda-Orjuela C, Castillo-Rivas J, Catalá-López F, Choi J, Christensen H, Cirillo M, Cooper L, Criqui M, Cundiff D, Damasceno A, Dandona L, Dandona R, Davletov K, Dharmaratne S, Dorairaj P, Dubey M, Ehrenkranz R, El Sayed Zaki M, Faraon E, Esteghamati A, Farid T, Farvid M, Feigin V, Ding E, Fowkes G, Gebrehiwot T, Gillum R, Gold A, Gona P, Gupta R, Habtewold T, Hafezi-Nejad N, Hailu T, Hailu G, Hankey G, Hassen H, Abate K, Havmoeller R, Hay S, Horino M, Hotez P, Jacobsen K, James S, Javanbakht M, Jeemon P, John D, Jonas J, Kalkonde Y, Karimkhani C, Kasaeian A, Khader Y, Khan A, Khang Y, Khera S, Khoja A, Khubchandani J, Kim D, Kolte D, Kosen S, Krohn K, Kumar G, Kwan G, Lal D, Larsson A, Linn S, Lopez A, Lotufo P, El Razek H, Malekzadeh R, Mazidi M, Meier T, Meles K, Mensah G, Meretoja A, Mezgebe H, Miller T, Mirrakhimov E, Mohammed S, Moran A, Musa K, Narula J, Neal B, Ngalesoni F, Nguyen G, Obermeyer C, Owolabi M, Patton G, Pedro J, Qato D, Qorbani M, Rahimi K, Rai R, Rawaf S, Ribeiro A, Safiri S, Salomon J, Santos I, Santric Milicevic M, Sartorius B, Schutte A, Sepanlou S, Shaikh M, Shin M, Shishehbor M, Shore H, Silva D, Sobngwi E, Stranges S, Swaminathan S, Tabarés-Seisdedos R, Tadele Atnafu N, Tesfay F, Thakur J, Thrift A, Topor-Madry R, Truelsen T, Tyrovolas S, Ukwaja K, Uthman O, Vasankari T, Vlassov V, Vollset S, Wakayo T, Watkins D, Weintraub R, Werdecker A, Westerman R, Wiysonge C, Wolfe C, Workicho A, Xu G, Yano Y, Yip P, Yonemoto N, Younis M, Yu C, Vos T, Naghavi M and Murray C. Global, regional, and national burden of cardiovascular diseases for 10 causes, 1990 to 2015. J Am Coll Cardiol 2017; 70: 1-25.
[33] Jeyabal P, Thandavarayan R, Joladarashi D, Suresh Babu S, Krishnamurthy S, Bhimaraj A, Youker K, Kishore R and Krishnamurthy P. MicroRNA-9 inhibits hyperglycemia-induced pyroptosis in human ventricular cardiomyocytes by targeting ELAVL1. Biochem Biophys Res Commun 2016; 471: 423-429.

[34] Platania C, PittalttaI Pascale A, Marchesi N, Anfuso C, Lupo G, Cristaldi M, Olivieri M, Lazzara F, Di Paola L, Drago F and Bucolo C. Novel indole derivatives targeting HuR-mRNA complex to counteract high glucose damage in retinal endothelial cells. Biochem Pharmacol 2020; 175: 113908.
[35] Yuan W, Liang X, Liu Y and Wang H. Mechanism of miR-378a-3p enriched in M2 macrophage-derived extracellular vesicles in cardiomyocyte pyroptosis after MI. Hypertens Res 2022; 45: 650-664.
[36] Liu N, Xie L, Xiao P, Chen X, Kong W, Lou Q, Chen F and Lu X. Cardiac fibroblasts secrete exosome microRNA to suppress cardiomyocyte pyroptosis in myocardial ischemia/reperfusion injury. Mol Cell Biochem 2022; 477: 1249-1260.
[37] Kaplan R, McGinn A, Pollak M, Kuller L, Strickler H, Rohan T, Cappola A, Xue X and Psaty B. Association of total insulin-like growth factor-I, insulin-like growth factor binding protein-1 (IGFBP-1), and IGFBP-3 levels with incident coronary events and ischemic stroke. J Clin Endocrinol Metab 2007; 92: 1319-1325.
[38] Wang J, Zhang J, Ma Y, Zeng Y, Lu C, Yang F, Jiang N, Zhang X, Wang Y, Xu Y, Hou H, Jiang S and Zhuang S. WTAP promotes myocardial ischemia/reperfusion injury by increasing endoplasmic reticulum stress via regulating mA modification of ATF4 mRNA. Aging 2021; 13: 11135-11149.
[39] Wen J, Lv R, Ma H, Shen H, He C, Wang J, Jiao F, Liu H, Yang P, Tan L, Lan F, Shi Y, He C, Shi Y and Diao J. Zc3h13 regulates nuclear RNA mA methylation and mouse embryonic stem cell self-renewal. Mol Cell 2018; 69: 1028-1038, e1026.
[40] Wang Q, Xie H, Peng H, Yan J, Han L and Ye G. ZC3H13 Inhibits the progression of hepatocellular carcinoma through mA-PKM2-mediated glycolysis and enhances chemosensitivity. J Oncol 2021; 2021: 1328444.
[41] Zhu D, Zhou J, Zhao J, Jiang G, Zhang X, Zhang Y and Dong M. ZC3H13 suppresses colorectal cancer proliferation and invasion via inactivating Ras-ERK signaling. J Cell Physiol 2019; 234: 8899-8907.
[42] Muscella A, StefStef.ysiologyG, Zhang X, Zhang Y and Dong M. ZC3H13 suppresses colorectal cancer proliferation and invasion American journal of physiology. Am J Physiol Heart Circ Physiol 2020; 319: H76-H88.
[43] Dankner R, Ben Avraham S, Harats D and Chetrit A. ApoE Genotype, lipid profile, exercise, and the associations with cardiovascular morbidity and 18-year mortality. J Gerontol A Biol Sci Med Sci 2020; 75: 1887-1893.
[44] Khan A, Mundra P, Straznicky N, Nestel P, Wong G, Tan R, Huynh K, Ng T, Mellett N, Weir J, Barlow C, Alshehry Z, Lambert G, Kingwell B and Meikle P. Weight loss and exercise alter the high-density lipoprotein lipidome and improve high-density lipoprotein functionality in metabolic syndrome. Arterioscler Thromb Vasc Biol 2018; 38: 438-447.
[45] Rahmati-Ahmadabad S, Shirvani H, Ghanbari-Niaki A and Rostamkhani F. The effects of high-intensity interval training on reverse cholesterol transport elements: a way of cardiovascular protection against atherosclerosis. Life Sci 2018; 209: 377-382.
[46] Farahnak Z, Chapados N and Lavoie J. Exercise training increased gene expression of LDL-R and PCSK9 in intestine: link to transintestinal cholesterol excretion. Gen Physiol Biophys 2018; 37: 309-317.
[47] Ahmad T, Chasman D, Buring J, Lee I, Ridker P and Everett B. Physical activity modifies the effect of LPL, LIPC, and CETP polymorphisms on HDL-C levels and the risk of myocardial infarction in women of European ancestry. Circulation. Circ Cardiovasc Genet 2011; 4: 74-80.
[48] Ayhan H, Gormus U, Isbir S, Yilmaz S and Isbir T. SCARB1 gene polymorphisms and HDL subfractions in coronary artery disease. In vivo 2017; 31: 873-876.